Korean J. Chem. Eng., **28**(7), 1625-1631 (2011)
DOI: 10.1007/s11814-011-0015-7

Controlling the morphology of trioctyl phosphine oxide-coated cadmium selenide/poly 3-hexyl thiophene composite active layer for bulk hetero-junction solar cells

Nguyen Tam Nguyen Truong*, Matthew Lowell Monroe, Umme Farva*,‡, Timothy James Anderson**, and Chinho Park*,†**

*School of Chemical Engineering, Yeungnam University, Gyeongsan 712-749, Korea
**Department of Chemical Engineering, University of Florida, Gainesville, FL 32611, U.S.A.
(*Received 19 December 2010 • accepted 18 January 2011*)

Abstract−Bulk hetero-junction solar cells with CdSe nanoparticles-P_3HT (poly 3-hexyl thiophene) composite active layer were fabricated, and the control of morphological feature of the nanoparticle-polymer composite thin films was investigated. A binary solvent composed of a primary solvent with intermediate polarity and a secondary solvent with high polarity was found to be effective in controlling the dispersion of the CdSe nanocrystals in the P_3HT matrix, and the modification of the nanocrystal surface by liquid-liquid extraction process was found to be effective in achieving the desired composite film morphology. Surface roughness of the active layer was optimized for various loadings of CdSe nanoparticles and could be reproducibly controlled to less than 10 nm.

Key words: Bulk Hetero-junction Solar Cell, Active Layer, CdSe Quantum Dot, Conjugated Polymer, Nanoparticle Dispersion

INTRODUCTION

Organic photovoltaics (OPV), which have been intensively investigated in the last two decades, have become promising as a next-generation solar cell which can realize both high-efficiency and low-cost photovoltaic energy conversion [1]. Multilayered organic materials are typically incorporated in these device structures, and the progress in device performance has been made by following the footsteps of the success of organic light emitting diodes (OLEDs) development. The highest efficiency reported for the OPV to date reached up to ~8%, where tandem device structure is incorporated [2,3]. However, the complexity of the fabrication process involved in these best performing cells hinders the commercialization of these novel devices.

The OPV has begun to gain a different outlook and widespread interest due to the recent development of bulk hetero-junction (BHJ) solar cells utilizing various materials systems [4,5], among which the BHJ solar cells constructed of the polymer-PCBM ([6,6]-phenyl-C_{61}-butyric acid methyl ester) blends [6] and polymer-nanocrystal blends [7] have been the most widely studied. The BHJ solar cells have an inherent merit in the simplicity of the fabrication process compared to that of the multilayered OPVs, for wet coating techniques such as screen printing or ink-jet printing could well be adapted for fabrication of BHJ solar cells.

The BHJ solar cells based on poly (para-phenylene vinylene) (PPV) derivatives (e.g. MEH-PPV, MDMO-PPV, etc.) and poly thiophenes (P_3HT, P_3OT, etc.) blended with PCBM have improved their cell efficiencies from 1% to 8% [8-10] by optimizing device structures and process conditions, including the introduction of interfacial carrier transport layers and a post-annealing process. However, the polymer-inorganic semiconductor BHJ solar cells have improved their cell efficiencies only up to 3% to date. Top efficiencies reported are 2.2% [11], 2.8% [12], 2.6% [13] and 3.13% [14] for solar cells utilizing hyperbranched, nanorods and tetrapods inorganic nanocrystals, respectively.

In the BHJ solar cells, p-type polymer acts as the light absorber, while PCBM or inorganic nanocrystals acts as the n-type electron transport material. The interfacial integrity between polymer and electron acceptors, bulk hetero-junction film morphology, and n-type acceptor loading and its distribution in the polymer matrix are among the key parameters affecting the efficiency of BHJ solar cells. The relatively lower efficiency of BHJ solar cells compared to that of multilayered OPVs is thus attributed partially to the morphology control of the active layer with respect to the intra-layer and inter-layer interfacial properties.

In the present work, cadmium selenide (CdSe) nanoparticles were synthesized and intermixed with the conjugated polymer, poly 3-hexyl thiophene (P_3HT), to form the active layer, and the effect of solution composition and thin film process conditions on the active layer morphology was elucidated and exploited in detail in an effort to improve the electron transport characteristics of the inorganic semiconductors in the polymer matrix. The BHJ solar cells also were fabricated with the developed optimized conditions and their device characteristics analyzed.

EXPERIMENTAL

We fabricated bulk hetero-junction solar cells by using P_3HT as the electron donor and CdSe nanocrystals as the acceptor in the following device structure: ITO/PEDOT : PSS/(CdSe+P_3HT)/Al. Each cell had an active layer area of ~4 mm^2, and a hole transparent layer

†To whom correspondence should be addressed.
E-mail: chpark@ynu.ac.kr
‡Current contact address: Research Center for Ultra Precision Sci. & Tech., Osaka University, Japan

Table 1. Tested solvents for the co-dissolution of P_3HT and nano-CdSe and their solubility characteristics

	Solvents	[a]M.W.	[b]B.P. (°C)	Polarity	Solubility of CdSe and P_3HT
Suitable	Chlorobenzene	112.56	131.7	2.7	Good
	Chloroform	119.38	61.2	4.1	Good
	O-dichlorobenzene	147	180	2.7	Good
	Toluene	92.14	110.6	2.4	Good
Unsuitable	Acetone	58.08	56.2	5.1	Poor
	2-Butanol	60.11	79.6	4.0	Poor
	MEK	72.11	80.0	4.7	Very poor
	Methanol	32.04	64.6	5.1	Poor
	Methyl ethyl ketone	114.19	144	4.0	Poor
	2-Propanol	60.11	82.4	3.9	Poor
	Pyridine	79.1	115.3	5.3	Poor
	THF	72.11	66	4.0	Fair
	Tetrachloroethane	167.85	146	-	Poor
	Benzene	78.11	80.1	2.7	Fair

[a]Molecular weight
[b]Boiling point

consisting of PEDOT : PSS on ITO (indium tin oxide) glass was used for hole collection, and the aluminum (100 nm) was used for the electron collection.

The P_3HT was purchased from American Dye Source, Inc., and poly(3,4-ethylene dioxyl thiophene) : poly(styrene sulfonate) (PEDOT : PSS) was purchased from Nanobest and was filtered through a 0.45 μm filter in air prior to use.

To find the proper solvent and its composition for the composite active layer and to achieve optimum performance, we performed an extensive search on suitable solvents, in which the solubility of P_3HT and dispersion of CdSe nanodots in the solution were primarily tested for all the candidate solvents. The list of solvents tested in this study along with their typical physical properties is summarized in Table 1. Selection of the candidate solvents was primarily based on their polarity index and boiling point.

The bulk hetero-junction active layers were formed by spin-coating the mixture of polymer and CdSe nanodots in the selected solvents, followed by vacuum-drying. The morphology of the active layer was first tested from single solvent. The formed active layer was analyzed and compared. Qualitative comparison of single solvent's performance on constructing the active layer is summarized in Table 1. Binary solvent mixtures using pyridine as the secondary solvent was then investigated for the improvement of active layer morphology. Surface morphology of composite active layer thin films was investigated by optical microscopy, scanning electron microscopy (SEM), atomic force microscopy (AFM), and surface profilometry.

CdSe nanodots of approximately 3 to 4 nm in diameter were used as n-type electron transport material, and the nanodots were synthesized in house following the procedure developed earlier [14,15]. The surface of the nanodots was naturally capped by TOPO (trioctyl phosphine oxide) during the synthesis procedure, where TOPO was introduced as a surfactant. The weight percentage of CdSe nanodots with respect to the polymer was kept constant at 60 wt-% for all the solutions prepared in this study. The composite solutions for comparative studies were prepared by changing the concentration of binary solvent mixture and loading amount of the solutes (CdSe +P_3HT) in the solution. The prepared solution was stirred overnight for 24 h at room temperature prior to use.

The ITO-coated glass was used as the substrate, and prior to film deposition the ITO surface was chemically cleaned by trichloroethylene (TCE), acetone and methanol with ultrasonification for 10 min successively followed by N_2 blow-drying. After being cleaned, the substrate was treated with N_2 plasma in a barrel-type plasma chamber for 10 min at a power of 50 W and a pressure of 200 mTorr. The PEDOT : PSS layer was spin-coated on the plasma-treated substrate with a typical thickness of 100 nm and vacuum-dried at 100 °C [16].

The active layer was prepared by spin-coating the composite solution onto the PEDOT : PSS deposited ITO substrate. The spin coating was done at 2,000-4,000 rpm for 30 sec, and the spin-coated film was dried under a vacuum at 65-120 °C for 30 min.

The I-V curves of fabricated solar cells were measured using a Keithley 2425 source measurement unit with an AM 1.5G solar simulator light source (100 mW/cm^2), and the power conversion efficiency determined.

RESULTS AND DISCUSSION

Fig. 1(a) and 1(b) depict the reasoning behind the solvent search experiments, where boiling point and polarity index of solvents were primarily taken into account. The polarity index is expected to be related to the solubility characteristics of the solutes in the chosen solvent, while boiling point is related to the thin film formation in terms of the rate of evaporation of solvents during vacuum-drying process. Solvents with a nearly constant polarity were selected in Fig. 1(a), and those with a nearly constant boiling point were selected in Fig. 1(b). Table 1 summarizes the physical parameters of these tested solvents as well as the results obtained from the solubility test experiments to choose the proper solvent for the co-dissolution of P_3HT and CdSe nanoparticles.

From the solvent survey experiments, it was found that the solu-

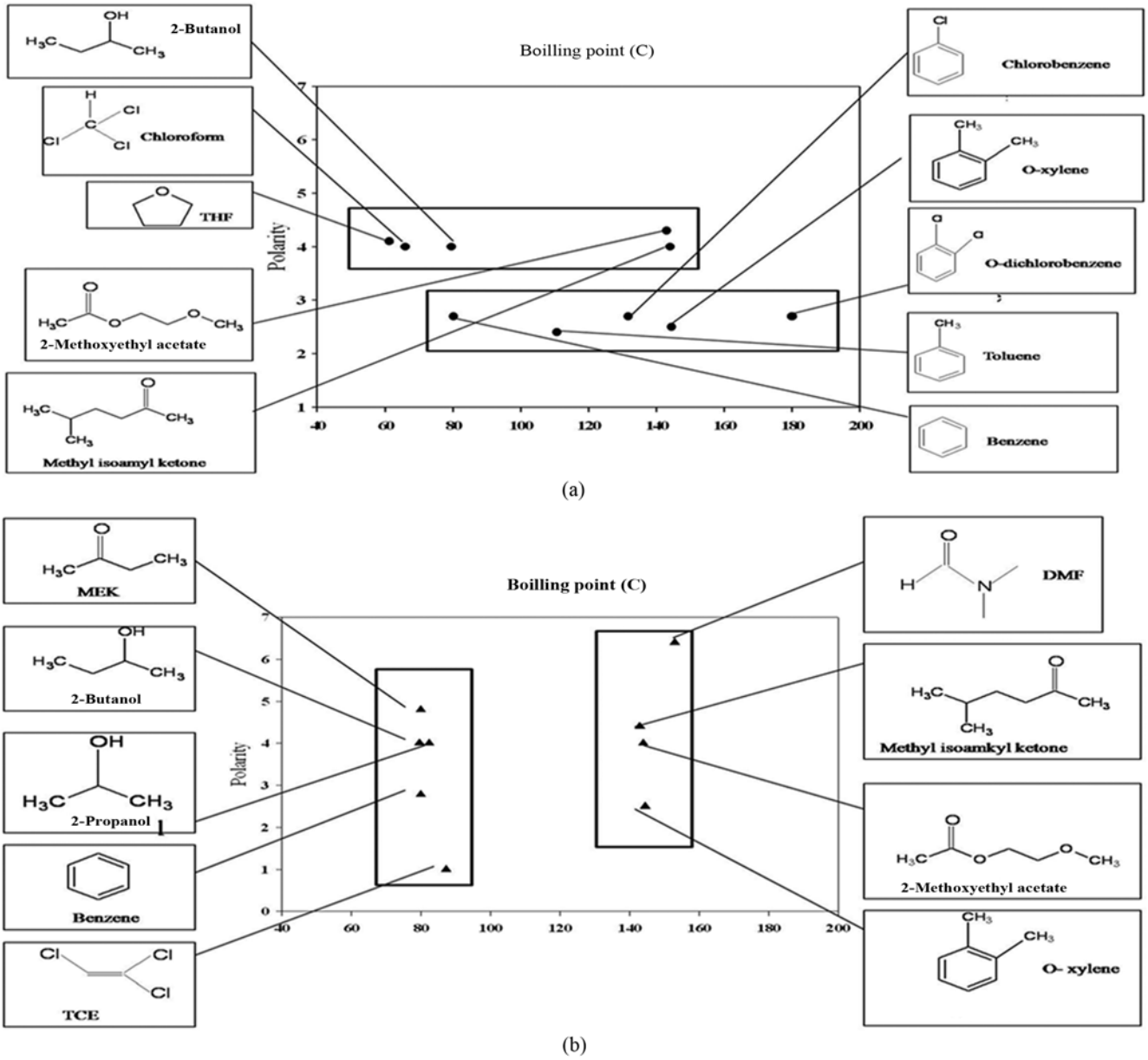

Fig. 1. Solvent selection diagram: (a) constant polarity group; (b) constant boiling point group.

bility of P_3HT strongly depends on the polarity of the solvent used. The P_3HT was insoluble in highly polar solvents and non-polar solvents, but soluble in the solvents of intermediate polarity such as chloroform and chlorobenzene [17]. The co-solubility characteristics of P_3HT and TOPO-capped CdSe mixture were tested for various solvents and compared in terms of surface roughness of the resulting thin film and nanoparticles' dispersion. The results are summarized in Table 1 and grouped as 'suitable' or 'unsuitable' solvents, where 'suitable' means that the solvent chosen dissolves both P_3HT and TOPO-coated CdSe very well, resulting in the composite active layer with good surface roughness and mono-dispersed nanoparticles in the polymer matrix.

The surface roughness and film morphology were investigated by optical microscopy, AFM and surface profilometry. The thin film morphology and surface roughness turned out to be the lowest in the films formed by using chlorobenzene or chloroform as the primary solvent. Therefore, these two solvents were chosen as the primary solvents in preparing the composite solution of this study.

It was also found that the addition of pyridine ('unsuitable' solvent having high polarity index) to chloroform or chlorobenzene enhances the nanoparticles' dispersion in the polymer matrix and improves the morphology of composite active layer significantly [18,19]. The concentration of secondary solvent (pyridine) was varied until it reached the solubility limit of the polymer (P_3HT), and the nanoparticle-polymer loading was also varied until it caused severe phase separation in the film. From a series of experiments where pyridine concentration in the solvent was varied as well as the loading of solute was varied, optimum solvent mixing conditions (typically less than 30% pyridine in volume) could be developed for chloroform and chlorobenzene.

Drying condition of spin-coated composite films was initially investigated at various temperatures ranging from 65 ºC to 140 ºC

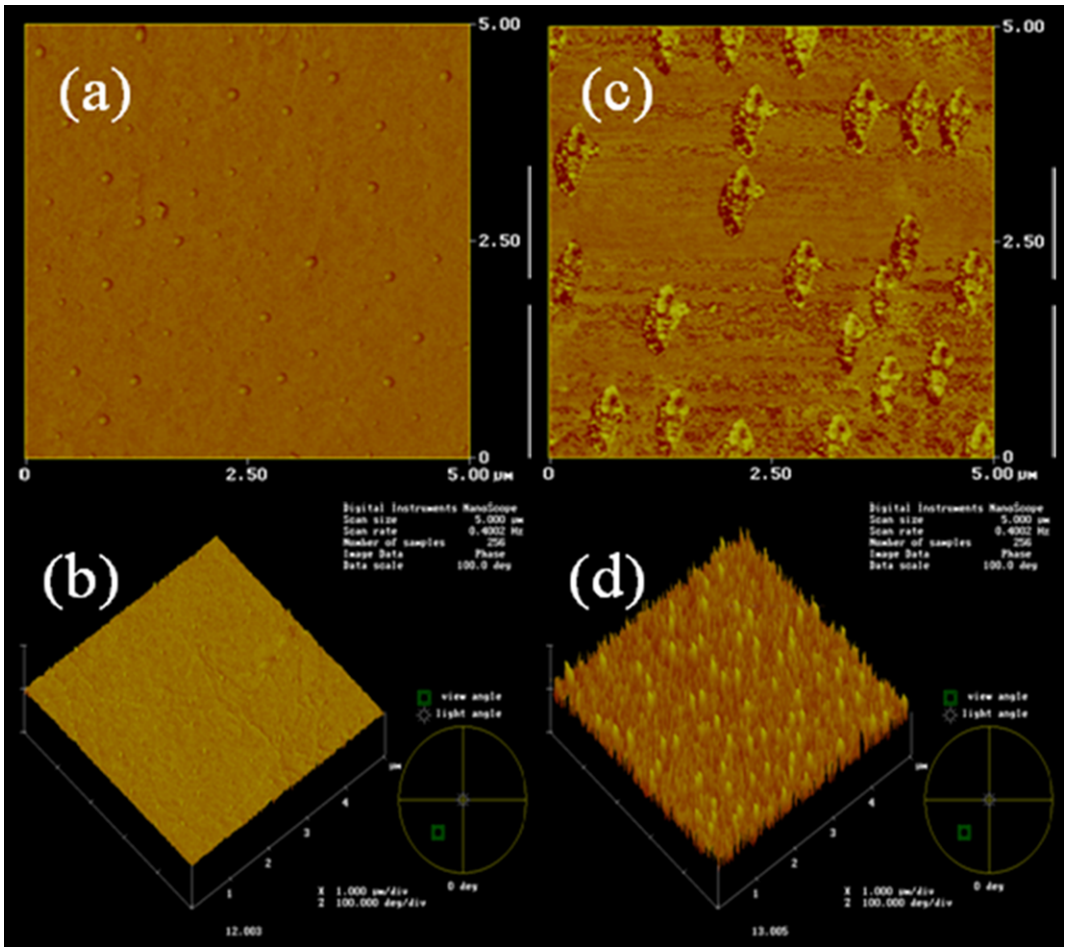

Fig. 2. AFM-TM topography images ((a) and (c)) and phase images ((b) and (d)) of the films consisting of 60 wt-% CdSe nanocrystals dispersed in P_3HT: (a) and (b) 30 vol-%; (c) and (d) 40 vol-% pyridine in chloroform. The total loading amount was kept at 5 mg/mL.

with a constant drying time of 30 min in a vacuum oven. It was observed that drying at 140 °C for 30 min provided a smooth and uniform surface without generating noticeable pinholes for the most of solutions investigated in this study.

Fig. 2 shows the AFM-Tapping Mode (TM) topography and phase images for 5 μm×5 μm scan areas of the CdSe-P_3HT blend films spun from binary solvent mixtures of 30% and 40% pyridine by volume in chloroform. At the higher pyridine concentration, the topography of the film becomes rough, whereas at the lower (and optimum) pyridine concentration, the film shows a much smoother surface. In the experiments of increasing pyridine concentration (Fig. 3), the increase of pyridine concentration up to 30% in chloroform solvent monotonically decreased the surface roughness of the resulting film. The AFM-TM phase images clearly show that the surface roughness is directly related to the phase separation behavior in the active layer. However, phase separation between the nanocrystals and polymer does not yield single material domains and, therefore, it is not possible to identify the individual polymer and nanocrystal areas in the thin films [19]. At pyridine concentrations of 30% and 40%, the RMS roughness was found to be 4.5 nm and 7.5 nm, respectively, for a solution loading amount of 5 mg/mL.

Fig. 3 shows the variation of the RMS surface roughness of the active layers with the pyridine concentration. The RMS roughness generally decreases with increasing pyridine concentration up to 30%, regardless of the loading amount, but the RMS roughness increases very rapidly when the pyridine concentration exceeds 30%.

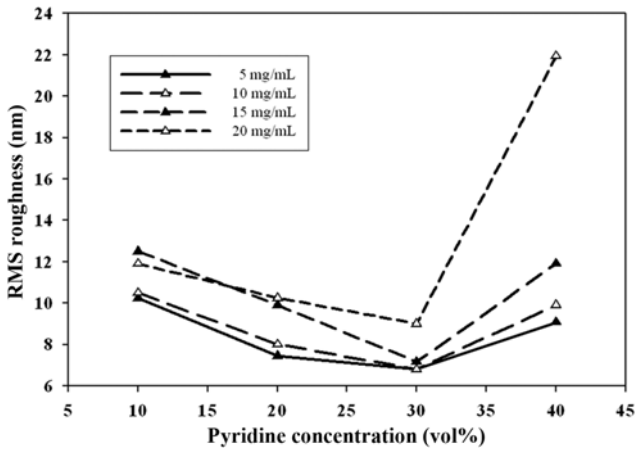

Fig. 3. Surface roughness of the films consisting of 60 wt-% nanocrystals dispersed in P_3HT as a function of the pyridine concentration in chloroform with different loading amounts in the solution.

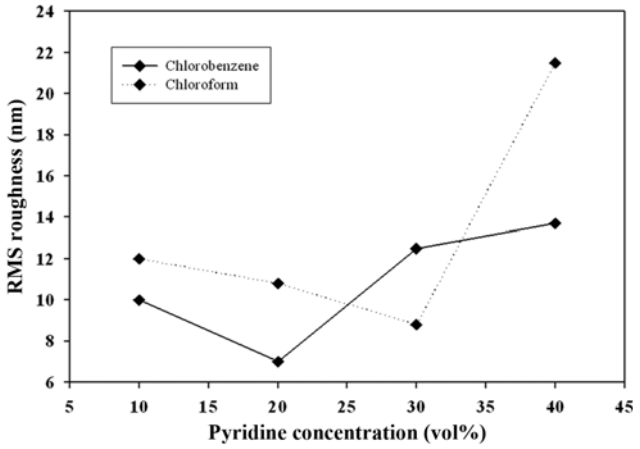

Fig. 4. Surface roughness of the films consisting of 60 wt-% nanocrystals dispersed in P_3HT as a function of the pyridine concentration with chlorobenzene and chloroform in solution.

As the pyridine concentration was at or above 40%, the polymer in the solution started to precipitate, because P_3HT is poorly soluble in pyridine.

The effect of the solute loading on the surface roughness was also studied, and it was observed that the roughness generally increases with the increase in solute loading as expected, but remains below 10 nm even for concentrations of up to 20 mg/mL when prepared with optimum binary solvent combination.

A binary solvent mixture using chlorobenzene as the primary solvent was also investigated and compared with the results of chloroform-based binary solvent. Fig. 4 shows that the surface morphology of the films obtained from the chlorobenzene-based binary solvent is superior to that of the films obtained from the chloroform-based binary solvent in terms of the added concentration of pyridine and surface roughness. Chlorobenzene-based binary solvent provided smoother surface morphology at lower amount of added pyridine. After the process optimization and reproducibility checks, the binary solvent with 20% pyridine in chlorobenzene was chosen as the optimized solvent combination for the fabrication of the BHJ solar cells of this study.

Fig. 5 shows that the thickness of film decreases with increasing spin-coating speed and increases with solute loading amount as expected. This result is believed to be caused by the hydrodynamic behavior of composite solution in which viscosity of the solution plays the major role. The film thickness could be reproducibly controlled in this study by adjusting the solute loading amount and spin-coating speed. From the horizontal sections of Fig. 5, the spin-coating speed to generate planned thin film thickness could be easily determined for different solute loading amounts. This can facilitate the future work regarding the device structure design and electrical and optical characterization of bulk hetero-junction composite thin films. The active layer thickness is an important factor in device performance: thicker active layers can harvest more photons, while thinner active layers have a smaller series resistance [20].

The surface of CdSe nanodots used mostly in this study was naturally capped by TOPO (trioctyl phosphine oxide) during the synthesis procedure as explained in the experiment section. The TOPO is, however, an electrical insulator; thus if it is not completely removed during the device fabrication processes, it could act as a resistance layer increasing the series resistance of the composite film. To improve the electrical conductivity of the active layers, we devised a method to convert the surface of CdSe nanodots from TOPO-capping state to pyridine-capping state, in which the liquid-liquid extraction process was utilized. Pyridine was selected because of its high polarity and compatibility with both CdSe nanodots and primary solvents used in this study, providing well-dispersed nanodots in polymer matrix. Both the electrical conductivity and co-solubility of nanodots and polymers in the primary solvent were expected to be improved by this surface modification of nanodots.

In the liquid-liquid extraction process, TOPO-capped CdSe was dissolved into pyridine and subjected to shaking for about 10 min, followed by the addition of n-hexane in the prepared solution. The mixture was then centrifuged for about 30 min. This process was repeated five times to remove the TOPO-surfactant from the CdSe nanoparticles and then vacuum dried to obtain the pyridine-capped CdSe nanoparticles.

Fig. 6 shows the dependence of RMS surface roughness of the resulting active layer containing pyridine-capped CdSe on the added

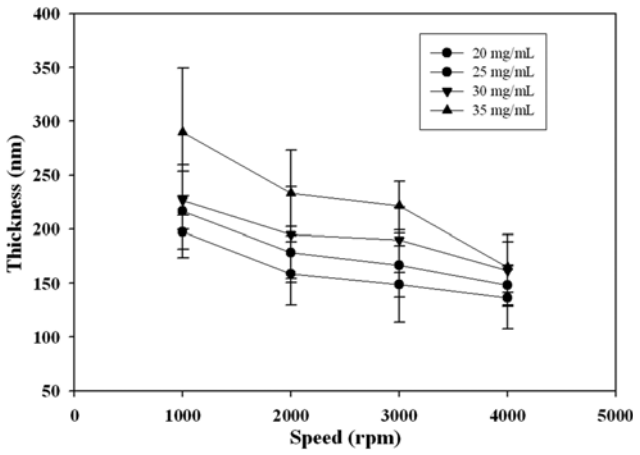

Fig. 5. The variation of the active layer thickness with the loading amount concentration and spin coating speed (rpm).

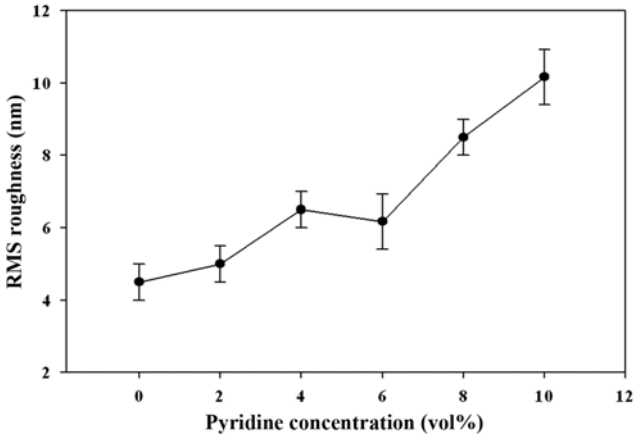

Fig. 6. RMS surface roughness of thin films made of pyridine-capped CdSe nanoparticle and P_3HT as a function of the pyridine concentration in chloroform.

pyridine concentration in chloroform solvent. As shown, surface roughness was well below 10 nm even without pyridine and it actually increased as the pyridine concentration was increased, as opposed to the results obtained in the case of TOPO-capped CdSe. Generally, the surface roughness obtained with pyridine-capped CdSe was superior to the one obtained with TOPO-capped CdSe, rendering a possibility of using single solvent. Further investigations are being made to exploit the process of using single solvent for BHJ solar cell fabrication, involving the characterization of electrical and optical properties of resulting active layer with respect to the solar cell performances.

The composite solution preparation condition for TOPO-capped CdSe nanodots was further optimized for fabrication of BHJ solar cells by varying the ratio of CdSe nanodots to P_3HT and added pyridine concentration. The optimized condition was obtained with 60 wt-% of CdSe with 20 vol-% of pyridine in chlorobenzene solvent.

Finally, the BHJ solar cells were fabricated by using the above optimized conditions. Table 2 shows the device characteristics at various loading amount of solutes, and it was found that the device efficiency increases with the solute loading amount. It was also found that percolation pathways for charge carrier transport could be developed in the active layer above the threshold solute (especially CdSe in the solute) loading concentration [21]. Fig. 7 shows the I-V curves of the fabricated devices, whose maximum efficiency reached to 0.12%. Further investigations are underway to improve the cell efficiency by incorporating post-annealing process after the Al electrode deposition to get rid of surfactant ligands on CdSe nanoparticle surface and to form lower resistance contacts, as well as utilizing the pyridine-capped CdSe nanoparticles with single solvent.

Table 2. Solar cell performance parameters (V_{oc}, J_{sc}, FF, η) vs. the loading amount of solute in the composite solution: Fixed conditions are 60 wt-% TOPO-capped CdSe; 20 vol-% pyridine in chlorobenzene solvent

Loading amount (mg/mL)	J_{sc}[a] (mA/cm^2)	V_{oc}[b] (V)	(FF)[c]	η (%)[d]
20	0.17	0.72	0.2	0.025
30	0.32	0.62	0.27	0.054
40	0.38	0.67	0.26	0.071
50	0.52	0.72	0.2	0.077
60	0.72	0.55	0.34	0.12

[a]Short circuit current density
[b]Open circuit voltage
[c]Fill factor
[d]Power conversion efficiency

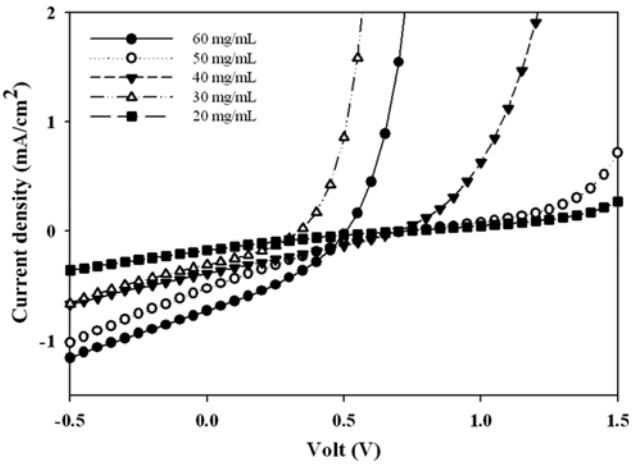

Fig. 7. I-V curves of fabricated bulk hetero-junction solar cells.

CONCLUSIONS

We investigated the preparation of composite solution and control of the morphology of active layers in detail to develop a reliable fabrication process for bulk hetero-junction solar cells containing TOPO-capped CdSe and P_3HT polymer. Chloroform and chlorobenzene were found to be viable candidates as the primary solvent for the composite solution. These solvents, with their intermediate polarity, were found to dissolve P_3HT very well. The binary solvent mixture formed by either of these solvents with the addition of pyridine was very effective in co-dissolving both P_3HT and TOPO-coated CdSe for a wide range of solute loading amounts. The obtained active layer apparently showed homogeneous mixing of CdSe nanodots in P_3HT polymer matrix with resulting root-mean-squares (RMS) surface roughness of less than 10 nm. The solute loading amount could be varied up to 60 mg/mL without seriously sacrificing the surface morphology.

ACKNOWLEDGEMENTS

This work was supported by Yeungnam University research grants in 2008, and the Human Resources Development Program (R&D Workforce Cultivation Track for Solar Cell Materials and Processes) of Korea Institute of Energy Technology Evaluation and Planning (KETEP) grant (No. 20104010100580), funded by the Korean Ministry of Knowledge Economy.

REFERENCES

1. W. C. Tang, *Appl. Phys. Lett*., **48**, 183 (1986).
2. P. Peuman, A. Yakimov and R. Forrest, *J. Appl. Phys*., **93**, 3248 (2003).
3. J. Y. Kim, K. H. Lee, E. N. Coates, D. Moses, T. Q. Nguyen, M. Dante and J. A. Heeger, *Science*, **317**, 222 (2007).
4. G. Yu and J. A. Heeger, *J. Appl. Phys*., **78**, 4510 (1995).
5. H. Hoppe and N. S. Sariciftci, Organic Photovoltaics, Taylor & Francis Group, Boca Raton, 217 FL (2005).
6. D. Chirvase, Z. Chguvare, M. Knipper, V. Parisi, V. Dyakonov and C. J. Hummelen, *J. Appl. Phys*., **93**, 3376 (2003).
7. C. N. Greenham, X. Peng and P. A. Alivisatos, *Synthetic Metals*, **84**, 545 (1997).
8. E. Shaheen, J. Christoph and S. Sariciftci, *Appl. Phys. Lett*., **78**, 841 (2001).
9. N. S. Sacriciftci, A. J. Heeger and F. Wudl, *Science*, **258**, 1474 (1992).
10. C. Y. Yang and J. A. Heeger, *Synthetic Metals*, **83**, 85 (1996).
11. I. Gur, N. A. Fromer, C. Chen, A. G. Kanaras and A. P. Alivisatos, *Nano. Lett*., **7**, 409 (2007).
12. B. Sun, H. J. Snaith, A. S. Dhoot, S. Westenhoff and N. C. Green-

ham, *J. Appl. Phys*., **97**, 014914 (2005).
13. B. Sun and N. C. Greenham, *Phys. Chem. Chem. Phys*., **8**, 3557 (2006).
14. S. Dayal, N. Kopidakis, D. C. Olson, D. S. Ginley and G. Rumbles, *Nano Lett.*, **10**, 239 (2010).
15. C. M. Donegá, P. Liljeroth and D. Vanmaekelbergh, *Small*, **1**, 1152 (2005).
16. U. Farva and C. Park, *Sol. Energy Mater. Sol. Cells*, **94**, 303 (2010).
17. Y. W. Kim, N. T. N. Truong, L. Monroe, T. J. Anderson and C. Park, *Korean J. Chem. Eng*., **25**, 1036 (2008).
18. W. Ma, C. Yang, X. Gong, K. Lee and J. A. Heeger, *Adv. Funct. Mater*., **15**, 1617 (2005).
19. M. L. Monroe, Y. W. Kim, N. T. N. Truong, Y. H. Na, L. J. Seo, T. J. Anderson and C. Park, Effect of Surface Modification by Solvent Exchange on Hybrid Bulk Hetero-junction Solar Cell Performance, *Materials Research Society Conference*, San Francisco, CA, U.S.A., 9-13, April (2007).
20. W. U. Huynh, J. J. Dittmer, W. C. Libby, G. L. Whiting and P. A. Alivisatos, *Adv. Funct. Mater*., **13**, 73 (2003).
21. P. Schilinsky, C. Waldauf and C. J. Brabec, *Appl. Phys. Lett*., **81**, 3885 (2002).
22. N. T. N. Truong, U. Farva, Y. W. Kim, Y. H. Na and C. Park, Controlling the Morphology of Nanocrystal-Polymer Composite for Bulk Hetero-junction Solar Cells, PVSEC-17, Fukuoka, Japan, 3-7, December (2007).